Computational Flow Dynamics Analysis of 5-holed Catalyst Geometries in Methane Steam Reforming

A Major Qualifying Project

Submitted to the Faculty of
Worcester Polytechnic Institute

In partial fulfillment of the requirements for the
Degree of Bachelor of Science
In Chemical Engineering

By

Matthew Carr

Date: April 2012

Dr. Anthony G. Dixon, Advisor

ABSTRACT

Steam methane reforming, also known as SMR is currently the leading source of hydrogen in the world's economy, producing at least 75%, if not more, of the world's hydrogen stock. In addition to being a very highly efficient process, it is currently the most cost-efficient way to produce hydrogen. These factors make SMR the leading contender for supporting a possible hydrogen economy. A typical SMR reactor contains a multitude of fixed bed tubes which contain catalysts pellets of varying size and geometry.

This project analyzed some new options for pellet geometry in SMR applications by using computational fluid dynamics software to model the behavior of three 5-holed geometries. This software analysis is necessary due to the high operating temperature of the reforming process which limits physical experimentation. Among the important qualities analyzed were pressure drop, heat transfer and methane conversion.

The specific geometries studied were designated 5H-P, 5H-P-small, and 5H-Q. It was determined that while 5H-P is the best option of these three, it does not perform much more efficiently than the currently produced 4H-Q model. However, it was proposed that a modified 5H-Q pellet may result in better performance under reactor conditions.

EXECUTIVE SUMMARY

Steam methane reforming, also known as SMR is currently the leading source of hydrogen in the world's economy, producing at least 75%, if not more, of the world's hydrogen stock. In addition to being a very highly efficient process, it is currently the most cost-efficient way to produce hydrogen. These factors make SMR the leading contender for supporting a possible hydrogen economy. A typical SMR reactor contains a multitude of fixed bed tubes which contain catalysts pellets of varying size and geometry.

The goal of this project was to analyze the performance of 5-holed cylindrical catalyst geometries in order to aid in the design of future reactor systems, which will in turn lead to more efficient SMR technology. The specific geometries studied were designated 5H-P and 5H-Q, with an additional 5H-P model studied with smaller holes.

The properties of an ideal catalyst include low pressure drop, so that a higher flow can be processed resulting in higher product output. In addition, the heat transfer within the reactor is highly important due to the high temperatures of the system. In addition to this the reactions of interest are highly endothermic and require high temperatures in order to maintain high conversion, so it is important that the entire reactor be maintained at a relatively uniform temperature. This requires efficient heat transfer due to the external heating of the reactor proper.

COMPUTER MODELING

In order to effectively study the behavior of the catalysts in a reactor environment, typically one would simply run a pilot-scale experiment. However, due to the high operating temperatures of the SMR reactors (often above 800K), these experiments are not feasible. Thus, it falls to computational fluid dynamics software to model the system and give insight as to what is happening in the system of interest. Specifically, a 120° periodic wall segment of the reactor was studied.

Meshes in this project were created with GAMBIT, and two separate FLUENT runs were performed for each particle geometry67 in order to model the system in the most accurate fashion. First, a flow-only run was performed in order to establish a more realistic inlet velocity profile. Using this, a reaction-enabled run was performed in order to model the species and heat transfer in the system.

RESULTS

After performing the FLUENT analysis, the results for the wall segment as a whole were studied. For the flow-only run, the pressure drop was specified at 3376 Pa/m, and each reaction run resulted in a calculated pressure drop similar to this value, though slightly lower. Mass flow rates increased with void fraction and tube wall temperatures as well as exiting gas temperatures remained relatively constant.

Following, the results for the test particle were analyzed in depth. Included here were values for particle surface area, heat sinks, and reaction rates. As expected, reaction rates were found to be highest in regions of high temperature as well as high methane flow due to the dependence of reaction rate on both temperature and concentration of methane. However, the 5H-Q case showed the highest reaction rates per surface area, despite having the lowest surface area of all three models.

Temperature contours of the three test particles near the tube wall were similar in features, though the 5H-Q case exhibited a much more intense temperature hotspot in one location in particular. This was shown to be the result of a higher fluid velocity and temperature near this location, resulting in more convective transfer at this point on the surface.

The flow fields of each case were relatively similar except for when analyzing flow impacting the bottom face of the test particle. It was seen that due to the orientation of holes on the base area of the particle, the 5H-P geometries tend to funnel more flow into the holes, whereas the 5H-Q deflects flow to the outer surface, where grooves tend to funnel it along the particle length. This causes the 5H-Q to have much better radial heat transfer and an overall more uniform temperature profile in the fluid.

CONCLUSIONS

The 5-holed particle geometries behaved quite similarly to each other, and also to a previously studied 4H-Q geometry. This was mainly due to similarities in void fraction, which governs several key factors such as pressure drop and mass flow rate. However, due to its higher void fraction and surface area, the 5H-P was the most effective of the three geometries studied. It was suggested that the 5H-Q could be modified in order to make it competitive with, if not superior to, the 5H-P geometry.

TABLE OF CONTENTS

TABLE OF FIGURES

TABLE OF TABLES

INTRODUCTION

Steam Methane Reforming, also known as SMR, is a commonly used industrial-scale process in which methane is converted into hydrogen and carbon dioxide through reaction with steam, usually at very high temperatures. SMR is the leading producer of hydrogen in the world, accounting for 80-85% of the world's hydrogen production in 2004[1]. SMR is a very energy efficient process, which typically varies between 65-75% efficiency, but can possibly reach higher values. Although the process costs are mainly dependent on the cost of natural gas to provide methane, it is still the most economically feasible option for hydrogen production. These characteristics make SMR the leading option for sustaining a viable hydrogen economy in future years.

SMR consists of three main reactions, which are summarized in Table 1 below, along with their respective reaction heats.

Table 1: Main Steam Methane Reforming Reactions

Reaction	Heat of Reaction (kJ/mol)
$CH_4 + H_2O \leftrightarrow CO + 3H_2$	-206.10
$CO + H_2O \leftrightarrow CO_2 + H_2$	41.15
$CH_4 + 2H_2O \leftrightarrow CO_2 + 4H_2$	-165.00

As noted previously, SMR reactors are often run at high temperatures (800-900K). This is mainly due to the endothermic heats of reaction for the first and third reactions in Table 1. By operating at higher temperatures, these reactions are more likely to occur spontaneously than at lower temperatures. This ensures a higher equilibrium conversion of the methane reactant, resulting in potential higher hydrogen production.

A typical steam reformer is comprised of a large number of smaller fixed-bed reactor tubes which are heated externally in order to maintain an appropriate process temperature. Within the reformer unit, a natural gas feed must be pretreated in order to remove any sulfur-based compounds. This step is necessary since sulfur atoms can easily poison the surface of any catalyst used in the steam reforming reactions to follow. The process results in removing a vast majority of sulfur content as gaseous H_2S.[6] (The most common catalyst used in SMR reactions is a cylindrical nickel-alumina (Al_2O_3) pellet which varies in shape and other features. A diagram of a steam reformer is shown in Figure 1.

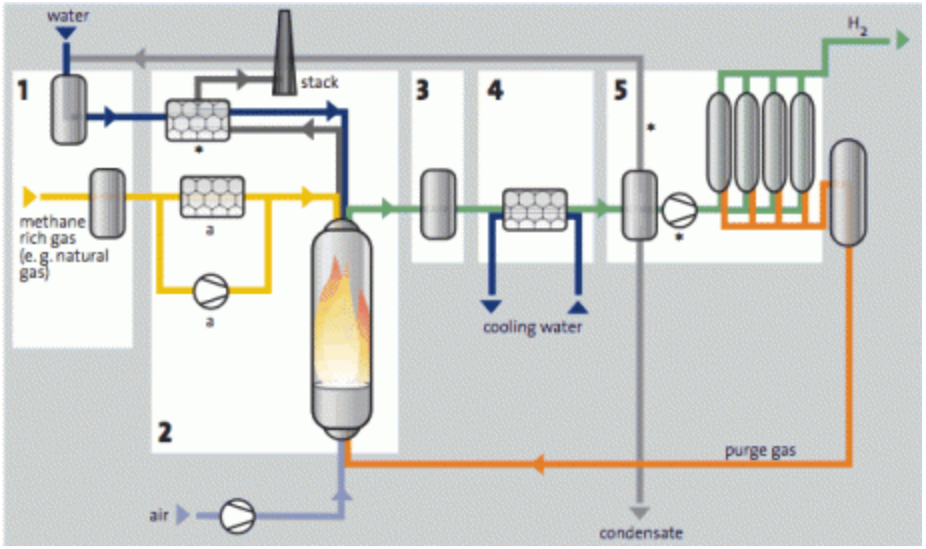

Figure 1: Steam reforming process diagram[8]

In order to effectively improve steam reforming processes, a better understanding of the inner working of the reactor beds is required. This involves studying the heat transfer properties and fluid dynamics of the process. For this purpose a Computational Flow Dynamics, or CFD, program is used to model the behavior inside the reactor. It is necessary to use computer simulation for this because the high operating temperature of steam reformers limits the amount of physical experiments that can be performed. In addition to these applications, CFD are also being applied to many other engineering models, many outside of chemical engineering, such as fire safety.[12]

The overall goal of this project is to analyze the performance of several 5-holed cylindrical pellet geometries under generic SMR reactor conditions.[11] This will allow for some insight as to the feasibility for using said geometries in industrial reactor applications. This will be achieved through a CFD analysis using the meshing program GAMBIT and the CFD software FLUENT. The following parameters will be used to determine the effectiveness of the various pellet geometries:

Heat transfer: Good heat transfer is desired due to the endothermic nature of the main reactions involved in this process. A large amount of heat is required to drive the reactions in the forward direction.

Pressure drop: Low pressure drop is desired, as it will allow for higher flow to be processed within the reactor without creating danger for the system and results in lower costs of running the reactor.

Methane Conversion: A high percent conversion for the reactants results in higher product concentration at the outlet of the reactor, and higher product quality. Also, by converting a higher

percent of reactants, it is possible to maintain product output with less feed or increase production with the current feed. In either case, this results in higher overall profit.

It is important to note also that although smaller catalysts generally increase available surface area, the resulting low void fraction creates a high pressure drop. Most SMR reactors require a lower pressure drop due to the high flow rates they process and thus use much larger particles which have holes and/or grooves to help increase surface area.[11] This is important because reaction generally only takes place on the particle surface for steam reforming, so maximizing surface area within a specific solid volume is of utmost importance.

In addition, this project seeks to compare the 5-holed geometries to the 4-Q geometry which is currently being produced and was studied with the same modeling software in a previous project.[7]

As in many applications, the major geometric characteristic which affects heat transfer and within a packed bed reactor is the ratio of surface area to volume. By incorporating a high surface area of catalyst into a relatively small volume, significantly more reaction sites are available, thus resulting in the reaction occurring more frequently throughout the reactor. The surface area is also more important as diffusion is highly limited in cases using catalysts because the reaction only takes place on the surface of the pellet.

On this topic, there has been a shift to use cylindrical pellets with multiple holes, since adding holes along the length of a cylindrical pellet will increase the available surface area without compromising structural integrity. Additionally, the holes serve a second function as the fluid can more easily flow through the bed as there are more paths to allow fluid flow. This also contributes to better mixing within the reactor bed as the holes will funnel flows in multiple directions and cause mixing upon exit.

This project uses the programs GAMBIT and FLUENT to model the various properties of the reactor system. GAMBIT is used in order to create the initial geometry and create a mesh for it, and FLUENT's multiphysics solver determines the various heat, reaction and flow properties of the system for specific conditions. The two basic geometries in this project are described below:

5H-P: This cylindrical pellet consists of 5 cylindrical holes in a pentagonal arrangement with 5 cylindrical grooves, or flutes, running along the outside staggered between the hole locations. The 5H-P model was also altered to a second case with smaller hole diameter (designated 5H-P-small)

5H-Q: This geometry consists of 5 cylindrical holes arranged in a cross along with 4 cylindrical grooves along the outside staggered with the 4 outer hole locations.

Figure 2 shows 3-D representations of the geometries studied.

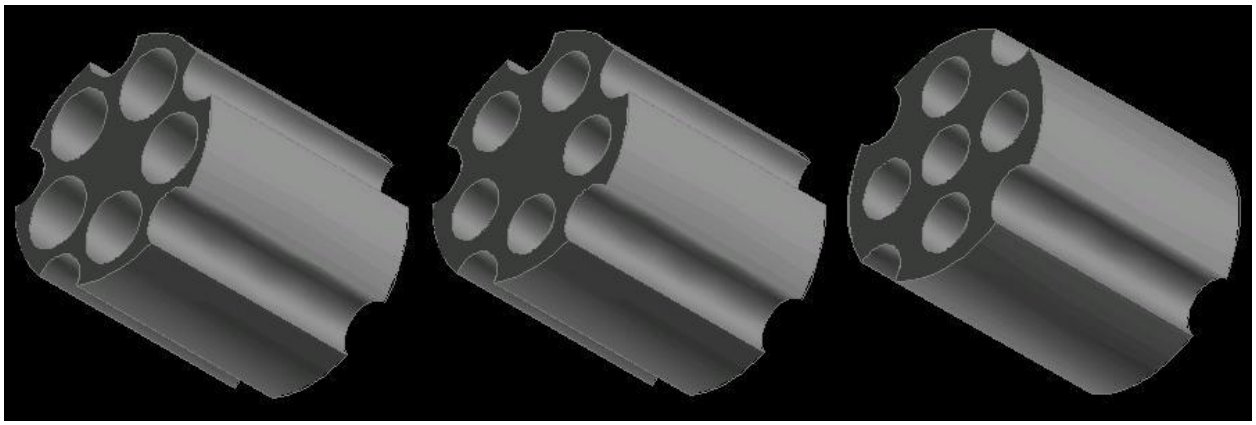

Figure 2: Individual particles for modeling. Left to right: 5H-P, 5H-P-small, 5H-Q

BACKGROUND

DESIRED REACTOR AND CATALYST PROPERTIES

This project focuses on the properties of the catalyst pellets being used in a steam reforming packed bed reactor tube. As such, it is important to note some of the important characteristics of a good catalyst material and geometry. Desirable characteristics are listed below, however it should be noted that these cannot all be optimized simultaneously, instead the best geometry is the one which encompasses the majority of these properties.

Low Pressure Drop: As stated previously, a low pressure drop allows higher flow rates of methane to be processed. This typically requires a high void fraction and thus larger particles which will generally leave larger spaces between them (less efficient packing).

High Surface Area: As previously mentioned, the majority of reaction which occurs takes place on the outer surface of the catalyst pellet due to limited diffusion within the pellet itself. By increasing surface area, more reaction can occur, resulting in higher conversion of reactants.

Structural Integrity: Due to the turbulent flow region in which the system is run at, the catalyst pellets must be able to handle the stresses of this as well as thermal stresses within the system. This property is not studied in this experiment, but it is worth noting that "weaker" particles are much less desirable because changes in the geometry of the pellets due to these conditions can adversely affect the operation of the reactor, such as increasing pressure drop.[2]

Radial Mixing: Since the temperature of the reactor tubes is maintained by external heating, it is important to have good mixing from the wall region to the center of the tube to maintain a more uniform temperature profile within the bulk flow. This can be measured by checking temperature profiles along the length of the reactor and comparing the fluid temperatures along the radial length of the model.

HEAT TRANSFER IN THE SYSTEM

In addition to the desired radial mixing, the remaining heat transfer areas in this system include:

Shell side heat transfer to the reactor wall: As noted previously, the temperature of the reactor is maintained through external heating, usually by radial heating in a furnace. It is important to maintain the reactor wall in a temperature range that positively affects the reaction kinetics. The tube wall also needs to be maintained at a nearly constant temperature in order to reduce thermal stresses within the system.

Transfer through the tube wall: Conductive heat transfer through the reactor wall is typically not a problem as most wall materials have high conductive heat transfer coefficients.

Fluid phase heat transfer: The heat transfers from the tube wall to the bulk fluid flow, heating the fluid to the desired reaction temperature. Poor convective heat transfer in this zone leads to higher tube wall temperatures and reduced tube life.[2]

Within the tube, the heat is transferred from the tube wall through the flowing fluid by means of convection. From the fluid, heat is taken in by the catalyst pellets in order to fuel the endothermic reactions in SMR.

CFD MODELING

Computational Flow Dynamics is a general class of computer modeling software which can be used in many engineering disciplines. Recent developments and improvements in computing resources and power have also allowed for the creation of more complex models which can be effectively solved. This leads to ever more accurate modeling of any and all systems desirable.

For this project, the desired geometry is essentially randomized packing of a fixed bed reactor. Considering the size of a normal reactor tube, it is much more convenient to reduce the size of the model. One problem that is often encountered in CFD simulations is obtaining a periodic flow condition, which is essential for establishing a realistic velocity profile at the inlet to the modeled section of tube. In CFD, this requires two identically meshed faces on opposite sides of the model. This seems simple enough, however in order to effectively model a packed bed reactor it is also desirable to create a geometry with somewhat random packing of pellets.

Fortunately, previous work has resulted in a geometry which conforms well to these restraints. A periodic wall segment of 120° with symmetry can effectively model the flow properties of the reactor.[10] The top and bottom faces are appropriately aligned for periodic flow conditions. The geometry being studied in this project can be seen in Figure 3.

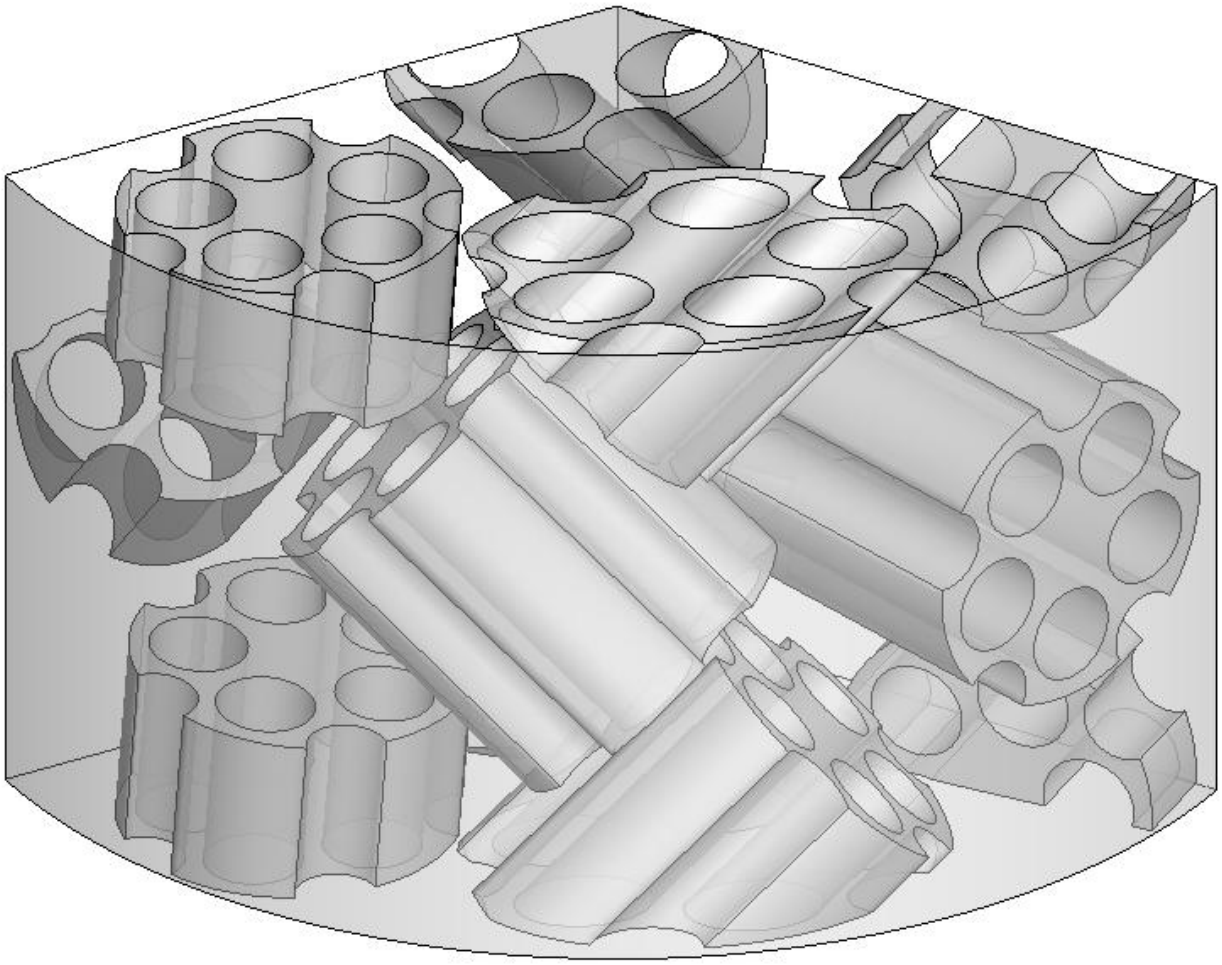

Figure 3: Reactor Wedge Geometry with 5H-P particles, viewed from outside tube wall

Turbulent Flow Modeling

In order to describe the flow occurring within the steam reformer reactor beds, an accurate model for turbulent flow is required. This is due to the high fluid velocities which are normally seen within the reactor beds (typically over 10 m/s). Previous models, such as the k-ε model, were unable to correctly show the behavior exhibited by this high velocity flow. Thus a more accurate model was required, and the recently developed SST k-ω model is much more capable of describing the overall flow patterns in this system. The main reason why other models fail to accurately model the flow in the fixed bed environment is the boundary layer area, which is poorly described by the k-ε model. The simple k-ω model does a much better job in the boundary layer regime, but is unable to model scenarios with more complex bulk flow. To this end, the SST k-ω model was developed, which essentially breaks the flow into two separate zones, a near-wall and a bulk flow region. SST k-ω uses a combination of the standard k-ω and k-ε models to describe the flow regions in which they are accurate, resulting in an overall more accurate description of the flow characteristics of the system.[5]

Diffusion

FLUENT is currently unable to model diffusion from the bulk fluid into catalyst particles defined as solid structures. Previous to the implementation of user defined functions in older FLUENT versions, multiple different attempts were made to more accurately model the transport at the fluid/solid interface. Previous studies attempted to model the solid particles as porous zones enclosed within a shell with bulk flow velocity of zero.[3] However, it was later determined that FLUENT does not apply a no-slip condition at the particle interface in this scenario, which does not follow the laws of fluid dynamics. For this project, in order to more accurately model the species mass fractions within the solid pellets, user defined functions/scalars were implemented though the use of a C file read into the FLUENT case.[9]

Reaction Kinetics

The accepted mechanism for SMR can be summarized by the following 9 elementary reactions in Table 2. Elementary steps 4-6 were considered to be the rate limiting steps in determining rate laws for this mechanism, developed by Hou and Hughes.[4]

Table 2: SMR mechanism

Step	Reaction
s1	$H2O+s\leftrightarrow H2+Os$
s2	$CH_4+3s\leftrightarrow CH_2s+2Hs$
s3	$CH_2s+Os\leftrightarrow CHOs+Hs$
s4	$CHOs+s\leftrightarrow COs+Hs$
s5	$COs+Os\leftrightarrow CO_2s+s$
s6	$CHOs+Os\leftrightarrow CO_2s+Hs$
s7	$COs\leftrightarrow CO+s$
s8	$CO2s\leftrightarrow CO2+s$
s9	$2Hs\leftrightarrow H2+2s$

The final rate equations determined by Hou and Hughes for the rate limiting steps in this mechanism are listed below. These equations were determined through the use of the Langmuir-Hinshelwood-Hougen-Watson (LHHW) approach.[4]

$$r_1 = \frac{k_1\left(\frac{P_{CH_4} * P_{H_2O}^{0.5}}{P_{H_2}^{1.25}}\right)\left(1-\left(\frac{P_{CO}P_{H_2}^3}{K_{P1}P_{CH_4}P_{H_2O}}\right)\right)}{DEN^2}$$

$$r_2 = \frac{k_2\left(\frac{P_{CO} * P_{H_2O}^{0.5}}{P_{H_2}^{0.5}}\right)\left(1-\left(\frac{P_{CO_2}P_{H_2}}{K_{P2}P_{CO}P_{H_2O}}\right)\right)}{DEN^2}$$

$$r_3 = \frac{k_3\left(\frac{P_{CH_4} * P_{H_2O}}{P_{H_2}^{1.75}}\right)\left(1-\left(\frac{P_{CO_2}P_{H_2}^4}{K_{P3}P_{CH_4}P_{H_2O}^2}\right)\right)}{DEN^2}$$

Where

$$DEN = 1 + K_{CO}P_{CO} + K_H P_H^{0.5} + K_{H_2O}\left(\frac{P_{H_2O}}{P_{H_2}}\right)$$

Each rate equation contains a term containing a k value and several partial pressures of species. The combination of these terms affects the overall rate of that reaction. This value is largely dependent on the heat of reaction and the temperature of operation. The remainder of the numerator represents the thermodynamic equilibrium of the reaction. This is the only term in the rate expression which can have a value of zero, at which point the reaction rate will be equal to zero and the reaction is at thermodynamic equilibrium. The denominator term, common to all three expressions represents the collective adsorption of all species on the catalyst.

In addition, the paper written by Hou and Hughes also summarizes the rate and equilibrium constants for these three reaction steps, which were found using the Arrhenius and van't Hoff equations, shown below.[4]

$$k_i = A_i e^{-\left(\frac{E_i}{RT}\right)}$$

$$K_i = A(K_i)e^{-\left(\frac{\Delta H_{i,a}}{RT}\right)}$$

Again, as FLUENT does not support reactions within solid phases, user defined subroutines were imported to the cases using a C file in order to describe the various solid properties of the species transport which occurs.

METHODOLOGY

GAMBIT MESHING PROCEDURE

The models used in this project are created based on a 120° wedge segment of a reactor bed which has been shown to give accurate results for a test particle.[10] This wedge is designed with symmetry planes and is identical on both the top and bottom faces, allowing for periodic boundary conditions in FLUENT. The wedge segment contains all or part of 12 distinct particles, which each contain 5 holes and either 4 or 5 grooves, depending on the specific model. Only one particle remains fully inside the wedge after the geometry is completed, and this particle is used as the test particle in the model. In addition, the ratio of tube to particle diameter was 4:1.

Individual Particles

To begin the creation of this geometry it is necessary to model a single particle. Three different catalyst geometries, which can be seen in Figure 2, were studied in this project, each measuring 1 inch in height with a 0.5 inch radius. The reactor wedge is modeled at a height of 2 inches with a 2 inch radius. The 5H-P particle contains 5 holes of 0.1434 inch radius in a pentagonal arrangement, with 5 0.12 inch radius grooves staggered between them along the outer edge. Additionally, another 5H-P particle was created with a hole radius of 0.12 inches in an attempt to study the effects of changing hole diameter on the system. This model was given the designation 5H-P-small. The 5H-Q model contains 5 0.12 inch radius holes arranged in an X across the particle, with 4 0.12 inch radius grooves staggered at 90 degree intervals. The previously studied 4H-Q geometry[7] contains 4 0.1434 inch holes in a square with 4 grooves of 0.12 inch radius staggered with the hole locations, similar to the 5H-Q but with the lack of the fifth hole.

Base Geometry

In order to complete the geometry for this study, the particle was copied eleven times and each one was individually translated and rotated to its proper position within the wall segment. The specific locations and rotations of these particles can be found in Appendix A.[10] The completed geometry in the 5H-P case is shown in Figure 4 below.

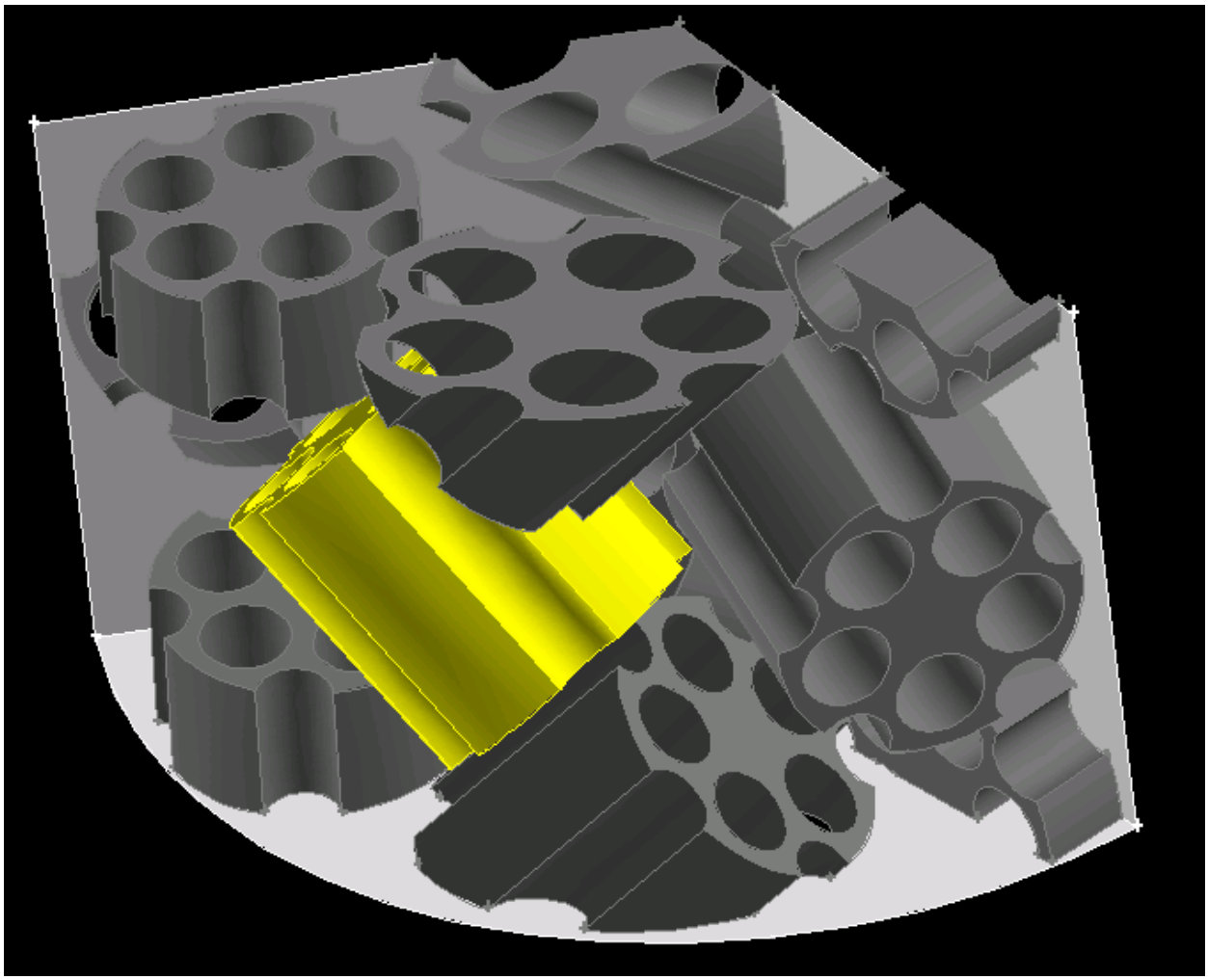

Figure 4: 5H-P reactor wedge geometry (test particle shown in yellow)

In order to clarify for future reference, each face was renamed according to which particle it was located on and whether it was a wall segment or a hole face. In this case, particle faces did not need connecting because when creating the original geometry, the reactor wedge cylinder was split with the individual particles instead of the particles being subtracted from the wedge.

Face Linking

In order to perform a periodic flow run in FLUENT, the corresponding top and bottom faces in the GAMBIT geometry must be linked together for meshing. This is due to a FLUENT requirement that periodic zones must have not only identical geometries, but identical meshes as well. Therefore, each individual face on the top and bottom of the reactor wedge were linked using a reverse orientation. This ensures that during the meshing step in GAMBIT, any given face on the top of the geometry will be meshed identically to the corresponding bottom face.

Boundary Layers

Boundary layers are added to some of the particles, as well as the outer wall of the reactor wedge. This helps to model the viscous layers and no slip boundary conditions at solid/fluid interfaces throughout the system. The most important are the ones added around the faces of the test particle in the model, as this will serve as the focus for the analysis and comparison of each particle type. GAMBIT requires three values when creating a boundary layer: the first layer size; a growth factor, which determines the ratio of the size of one layer to the next; and the total number of layers. In the models for this project, the first layer has a height of 0.005 inches and a growth factor of 1, meaning that all layers have the same thickness. On the test particle, the 5H-P uses only 2 layers, since using anymore results in overlap of the boundary layers inside the particle volume. The other 2 models use 4 layers due to more available space between particle surfaces. Details about the various boundary layers used in the GAMBIT meshes can be found in Appendix B.

Meshing the Model

Finally, after adding boundary layers to the geometry, the entire model was meshed using tetrahedral elements with an edge length of 0.03 inches. In order to properly mesh the entire model, certain faces were pre-meshed to avoid problems when meshing the entire fluid volume. These faces vary between the three models, but are normally located in regions with small volumes, usually near the symmetry planes of the model. All the solid particle zones as well as the fluid zones were meshed completely as it is necessary to model within both phases. Figure 5 below shows the 5H-P mesh for the solid particles only.

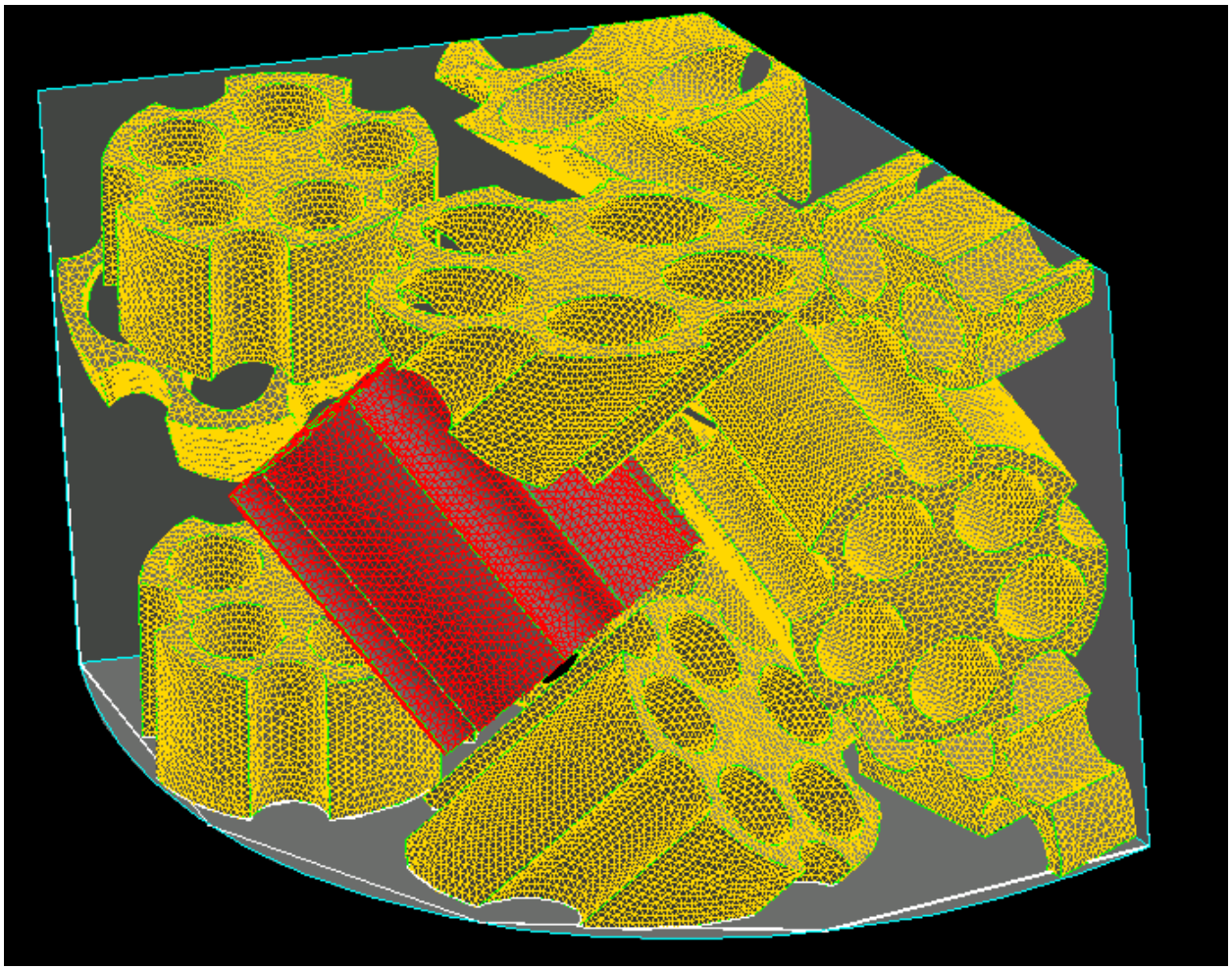

Figure 5: Meshed Model for 5H-P geometry (test particle mesh in red)

FLUENT: CFD MODELING PROCEDURE

Flow Only Run

For the first run for each geometry, the solver is run only for the flow equations in order to develop an appropriate inlet velocity profile. This requires the use of periodic flow conditions.

Initial Setup

After opening the imported mesh file from GAMBIT, the mesh is scaled to the appropriate units since FLUENT defaults to meters, where GAMBIT uses inches. The various FLUENT models are then chosen. In this study, all solution models use the Green-Gauss Node based solver and are time-independent. In addition the energy equation is used in addition to a reaction model, along with the SST k-omega model including transitional flows.

Reactor Conditions

The reactor operating conditions are taken from the previous MQP on which this study is based and are summarized below in Table 3.

Table 3: Reactor Wall Segment Conditions

Reactor Conditions			
Inlet Flow Temperature (K)	Reactor Wall Heat Flux (kW/m^2)	Operating Pressure (kPa)	Inlet Flow Velocity (m/s)
824.15	113.3	2,159	3.2
Fluid Properties			
Heat Capacity (J/kg-K)	Thermal Conductivity (W/m-K)	Viscosity, M (Pa-s)	
2395.38	0.0876	3E-05	
Solid Properties			
Density (kg/m^3)	Heat Capacity (J/kg-K)	Thermal Conductivity (W/m-K)	
1947	1000	1	

The fluid properties above describe the reacting gas mixture flowing through the tube segment which contains methane, hydrogen, carbon monoxide, carbon dioxide, and water vapor. The various properties of each species in this mixture are summarized below in Table 5. The solid material used for the 12 particles is alumina (Al_2O_3).

Boundary Conditions

The basis for FLUENT's solutions are the boundary conditions set by the user to describe the behavior of the system at various interfaces. For this model, the majority of the boundary types were defined as WALL boundaries during the GAMBIT procedure. For the purposes of fluid flow, this results in a no-slip condition at each fluid/solid interface. The periodic condition is set for a specific pressure drop between the inlet and outlet locations. For these models, the set pressure drop was 3376 Pa/m. Each wall boundary was also set to the appropriate solid material alumina, for which the properties are described above.

Solution Initialization and Iteration

In order to begin developing a solution, FLUENT requires a starting point, much like the need for an initial condition when solving a differential equation. In this case, FLUENT needs values corresponding to values in the viscous model, as well as a temperature and inlet velocity profile. Table 4 summarizes the initialization conditions used for the flow runs.

Table 4: Initialization conditions for flow runs

Temperature (K)	Inlet Velocity (m/s)	Turbulent Kinetic Energy (m^2/s^2)	Specific Dissipation Rate (s^{-1})
824.15	3.2	0.256	43000

After initializing, FLUENT allows the user to choose a number of iterations to perform. FLUENT also has built-in criteria for convergence in the form of residuals which can be used to approximate when a solution will remain unchanged through further iteration. Should the solution reach a point where all residuals are below the specified or default values for convergence, the solution process will halt and a message will be displayed stating that the solution has converged after however many iterations have been performed. For these flow only runs, the solutions generally converged within 1000 iterations based on the default residual settings.

Final Steps

In order to ensure the convergence of the solution, it is advised to check that mass and energy balances are closed within a reasonable amount. This is easily achieved through FLUENT's flux reports function, which is capable of calculating mass flow rates, as well as heat transfer rates through one or more surfaces present in the model. After confirming that the solution is significantly converged, the velocity profile for the outlet of the model was saved to be used as the inlet profile for the reaction run.

Reaction Run

After completing the flow only run, the mesh was reloaded into FLUENT, along with the previously saved inlet flow profiles. The beginning steps for setting up this solution are similar to those described for the flow only run, with a few additions. In addition, the models for multicomponent mixtures are enabled in order to correctly model the species transport that occurs.

Initial Setup

For the reaction case, it is necessary to interpret a premade C file which contains user defined subroutines that will calculate the species compositions and reaction rates within the solid particles. This is necessary because FLUENT is not capable of performing reactions within solid zones of a model. Therefore the C file is created with various functions which can be used to have FLUENT calculate the

desired quantities. Also incorporated in the C file is a subroutine to calculate the total heat sink of the test particle, and this is used not only for results but also convergence purposes.

Reactor Conditions

The conditions for the overall model have additions from the flow only run, including the initial mass fractions of the various components, as well as additional diffusivity data based on the user defined functions for reactions within the system. Detailed below in Table 5 are the various additional conditions set for the fluid mixture and solid material properties. Note that in FLUENT, the user scalars are a separate entity from species, and the numbers in this table show which species each user scalar represents. Note also that water vapor is present in the mixture, which is why mass fractions do not sum to one.

Table 5: Diffusivity and mass fraction values for species in fluid mixture.

User Scalar Number	Species	Mass Diffusivity (m^2/s)	Mass Fraction
0	Methane	1.23 · 10-5	0.1966
1	Hydrogen	2.25 · 10-5	0.0005
2	Carbon monoxide	7.2 · 10-6	0.0007
3	Carbon dioxide	4.9 · 10-6	0.1753

The mass diffusivities above are used in order for FLUENT to determine the overall diffusivity of the fluid mixture. In addition, the user defined functions are linked to the diffusivities of each user scalar in order to determine their diffusivity values within both the fluid and solid zones of the model.

Boundary Conditions

In the setup of the reaction run, the boundary conditions for the model change drastically to account for the addition of reacting species to the reactor wedge. To begin, the bottom and top zones are changed to a velocity inlet and a pressure outlet respectively. The velocity profile from the flow run is used here to describe the incoming fluid flow. The pressure outlet is set at zero gauge pressure and backflow is enabled.

For species transport across the fluid/solid interfaces, there are a variety of boundary conditions which must be set in order to model the transfer correctly. Since FLUENT does not account for species within solid zones, the condition is set for no diffusive flux across the solid walls. However, the user defined scalars have values within both solid and fluid. This requires a constant value condition at the wall to maintain continuity of value and diffusive flux across the boundary. The value is defined according to a specific subroutine, which will maintain that the value near the wall remains equal in the fluid and solid cells near the boundary.

Solution Initialization and Iteration

As in the flow only run, the solution must be given a starting point, thought there are a few additional values that must be specified for this specific simulation. Each species must be given an initial mass fraction as well as the values for user defined scalars.

In order to run the simulation without causing any problems with methane depleting in the system, the solution is iterated in three steps, with only one change in between each step. One of the first lines in the C file defines a solid density, rho, on which the reaction rate functions are based. By lowering this value, the magnitude at which reactions proceed is greatly reduced, resulting in a drop in methane consumption within the simulation. In order to iterate the solution without initially depleting all the methane in the system, it was necessary to use a bootstrapping procedure, which involved running several iterations with rho at 1% and 10% of its actual value, before running several hundred iterations at the full value.

Solution Convergence

The use of residuals is unlikely in this simulation to give a good idea of when the solution is converged. This is due to the use of the user defined functions and subroutines within the C file. Instead, additional convergence criteria are used in the form of mass and energy balances. By using the flux reports function in FLUENT, a simple check can be made on the overall heat and mass balance in the system.

Additionally, there were a few user defined functions which could be used to check the agreement between FLUENT's solutions and the reaction models found in the C file. The first of these is a heat sink calculation for the test particle. This will determine the amount of heat absorbed by the test particle due to reaction conditions. This value can be compared with the FLUENT flux report for heat transfer rate over the various surfaces of the test particle. Secondly, two user defined functions were available which calculate reaction rates inside the test particle as well as species flow within the test particle. By comparing the reaction rates and species flow with the help of stoichiometry, the mass balance on the test particle can be easily confirmed.

Final Steps

After the solution is sufficiently converged, it is then possible to move on to the various post processing features contained in the FLUENT engine. These allow for the display of temperature or species concentration plots over various surfaces, as well as flow pathlines, etc.

RESULTS

The most basic results can be seen in Tables 6 and 7 below, which summarize some values of interest for the reactor wedge and test particle for each of the three geometries. Additionally, the corresponding results from the previously studied 4 hole grooved case are included as a reference.

Table 6: Results for Reactor Wedge

Geometry	Void Fraction	Pressure Drop (Pa/m)	Mass flow Rate (kg/s)	Average Tube Wall Temp. (K)	Average Temp. of Exiting Gas (K)
4H-Q[7]	0.72	3285	0.03812	1062.0	827.0
5H-P	0.77	3167	0.03837	1064.0	827.3
5H-P small	0.71	3300	0.03642	1064.7	827.4
5H-Q	0.70	3360	0.03734	1064.5	826.1

Table 7: Results for Test Particle

Geometry	SA (m^2)	Average Surface Temp (K)	Total Heat Sink (W)	Surface Heat Flux (W)	Methane Flow (kmol/s)	Rxn Rate 1 (kmol/s)	Rxn Rate 2 (kmol/s)	Rxn Rate 3 (kmol/s)
4H-Q[7]	0.00520	803.3	64.85	64.77	-3.88E-7	2.18E-8	-6.06E-9	3.64E-7
5H-P	0.00574	804.9	64.14	64.04	-3.83E-7	2.21E-8	-6.42E-9	3.60E-7
5H-P small	0.00539	805.0	61.50	61.26	-3.68E-7	2.13E-8	-6.12E-9	3.45E-7
5H-Q	.00534	803.7	64.22	64.10	-3.84E-7	2.16E-8	-5.67E-9	3.61E-7

The results show that the 5-holed geometries behave quite similarly to the 4H-Q particle on average. However, average values can often be skewed by a wider range of values over the entire domain, so it is important to make sure that the overall model is analyzed for slight differences that may be more relevant.

There are some observed trends in the numeric results tabulated above. As expected, with increasing void fraction, there is a proportional decrease in pressure drop as the fluid takes on average a shorter path through the tube segment. However, as the pressure drop changes, it differs more from the prescribed value of 3,376 Pa/m which is designated as the actual pressure drop in the flow only runs. This can be explained by a few things. One is that due to reaction, the molar flow rate changes due to the stoichiometry of the reaction. This results in changes in total pressure of the exiting fluid. Secondly, the written velocity profiles are simply a series of points and not a continuous function. Naturally, interpolation will induce some amount of error and result in some deviation from expected values.

Additionally it is seen that the particle surface temperature is slightly higher in the 5H-P cases. It is likely that this is due in some way to the additional groove on the outer surface, as the 4H-Q and 5H-Q have similar values which are both lower than the 5H-P case.

Though the tube wall temperature does not vary greatly from one model to the next, it is important to note that it is slightly higher than the value from the 4H-Q model. Higher tube wall temperatures generally result from poor convective heat transfer near the tube wall, probably from reduced flow. The implications of higher tube wall temperatures are increased thermal stress for the entire system, which can lead to a shorter lifespan of the equipment.

Also important is that numerically, there are no major changes between the 5H-P and 5H-P-small cases, implying that hole diameter does not have a large effect on the behavior of the system. This implies that larger holes would be preferred due to higher surface area and void fraction, which in turn allow for lower pressure drop.

TEMPERATURE FIELD COMPARISONS

The main points of interest in studying these three potential geometries are things that differ between them, not simply analyzing the various numerical data that result from the simulations. As was found in previous work[7], the test particle shows an intense hotspot in one area near the tube wall. The intensity of this hotspot was found to increase with increasing void fraction in the model. However, this trend was broken when looking at the 4 hole grooved case, where the hotspot was much less intense despite a significantly higher void fraction.[7] In order to determine whether or not the newer geometries are “better” than the 4 hole grooved model, the temperature contours for the test particle are shown in Figure 6.

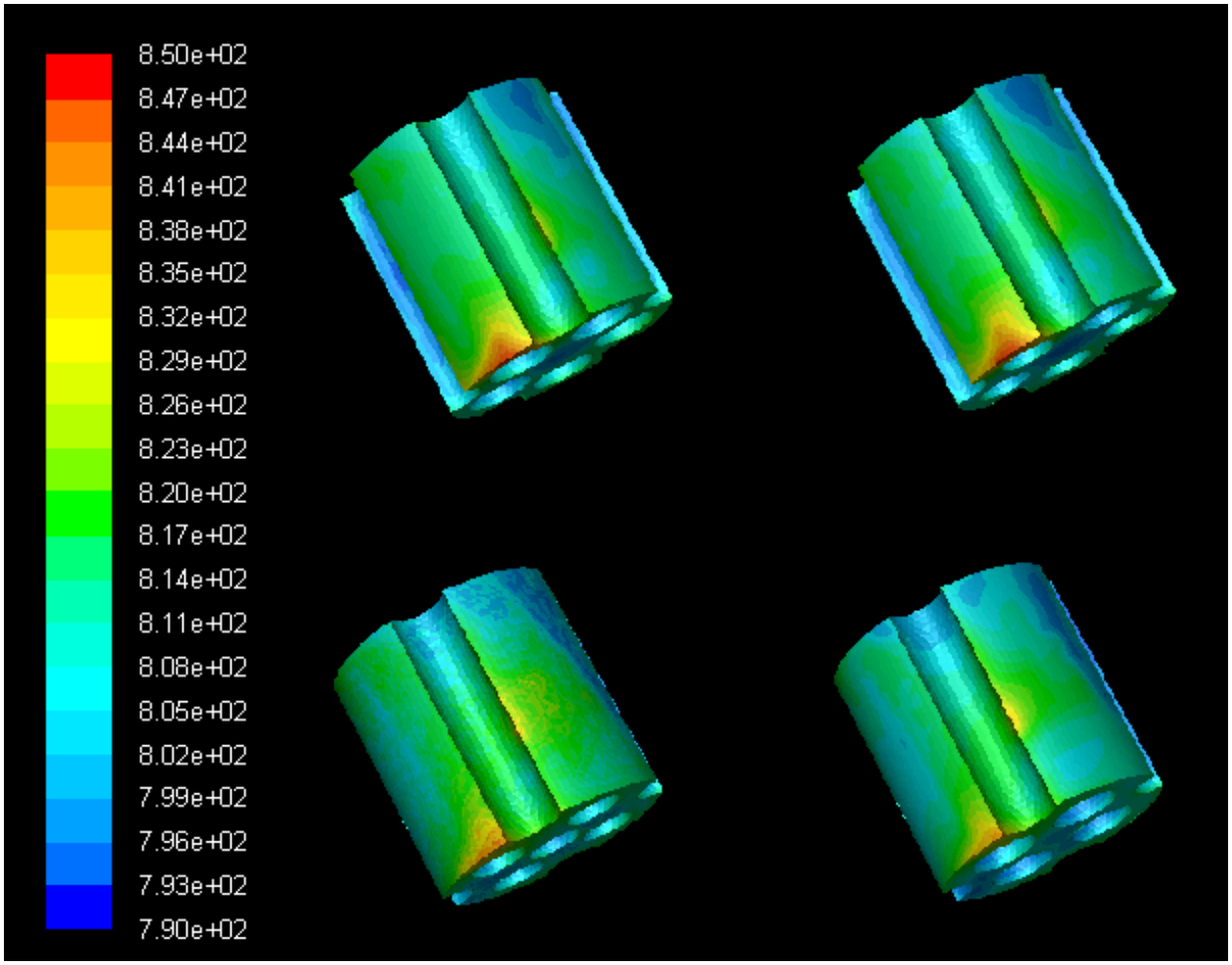

Figure 6: Temperature fields top-left 5H-P, top-right 5H-P-small, bottom-left 5H-Q, bottom-right 4H-Q

In the three 5 holed geometries, the hotspot is indeed present and visual comparison shows that the trend with increasing void fraction is followed, since the 5 hole cases have similar or slightly higher void fractions than the 4 hole case and the intensity of hotspots corresponds accordingly. Of note when comparing the temperature contours is that the 5H-Q case has a second, smaller hotspot area on the right side of the visible groove in Figure 6. The question is not necessarily why this spot is warmer than in the 5H-P cases, which have higher void fraction but why the second hotspot exists solely in this specific geometry.

On further inspection, a low intensity hotspot is visible in the two 5H-P cases, but the difference in temperature magnitude from the surrounding area is much less noticeable than in the 5H-Q model.

REACTION RATE COMPARISONS

In figures 7 and 8, the reaction rates on the test particle surface for reactions 1 & 3 are shown. In order to make any sort of quantitative comparison it was necessary to scale all four models to the same range of values. By doing this, it is easily seen that the 5H-Q geometry has generally higher reaction rates over the entire particle surface, including two areas of very high reaction rate. These two

areas correspond to the temperature hotspots shown by the temperature contours in figure 6. This is expected as all reactions will have increased rate at higher temperature.

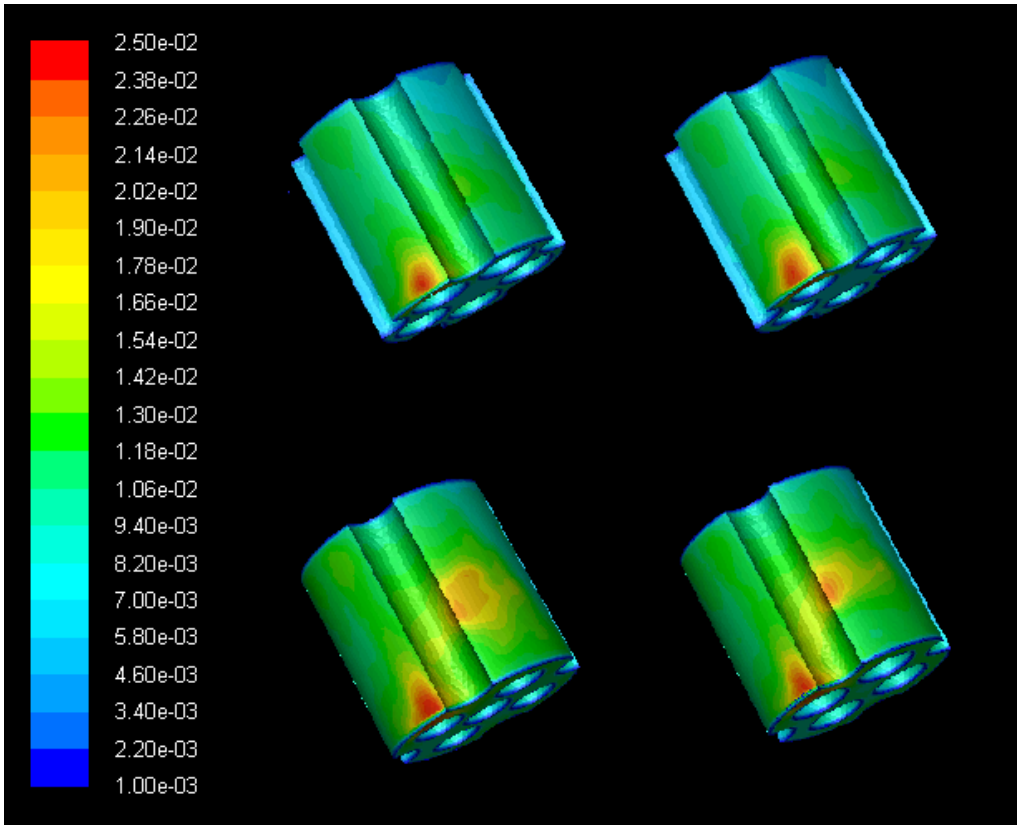

Figure 7: Reaction Rate 1 Contours: Top-Left 5H-P, Top-Right 5H-P-small, Bottom-left 5H-Q, bottom-right 4H-Q

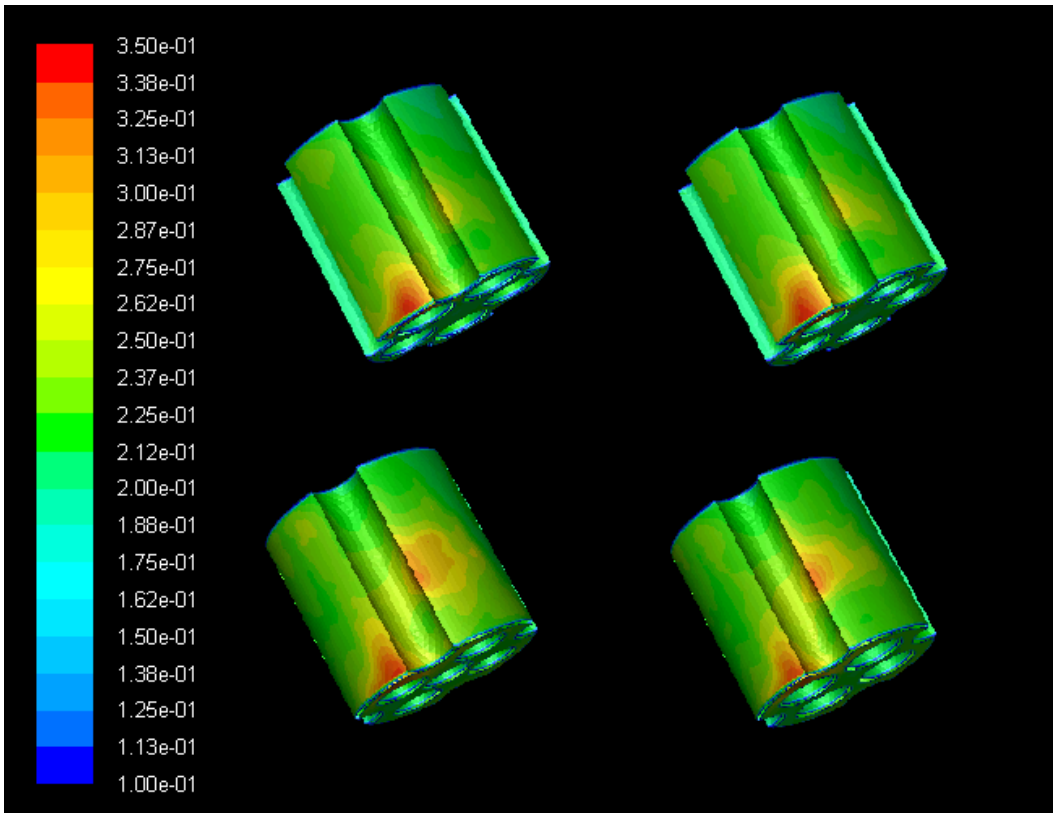

Figure 8: Reaction Rate 3 Contours: Top-Left 5H-P, Top-Right 5H-P-small, Bottom-left 5H-Q, Bottom-right 4H-Q

Typically when looking at a reaction taking place on a catalyst in steam reforming, the reaction occurs more with increasing external surface area of the catalyst over which the reacting mixture flows due to limited diffusion, which inhibits the use of internal surface area for reaction. However, the opposite is occurring in this experiment. The 5H-Q geometry has the lowest surface area of the three models, however the rate of reaction 3 has its highest value in this case. However, note that the temperature of the test particle in this case is also higher than in both 5H-P models, which explains why the reaction will proceed more quickly. The question then remains why the temperature in the 5H-Q geometry is higher than in other models.

METHANE CONVERSION

Contour plots for the mass fraction of methane in the test particle are shown in Figure 9.

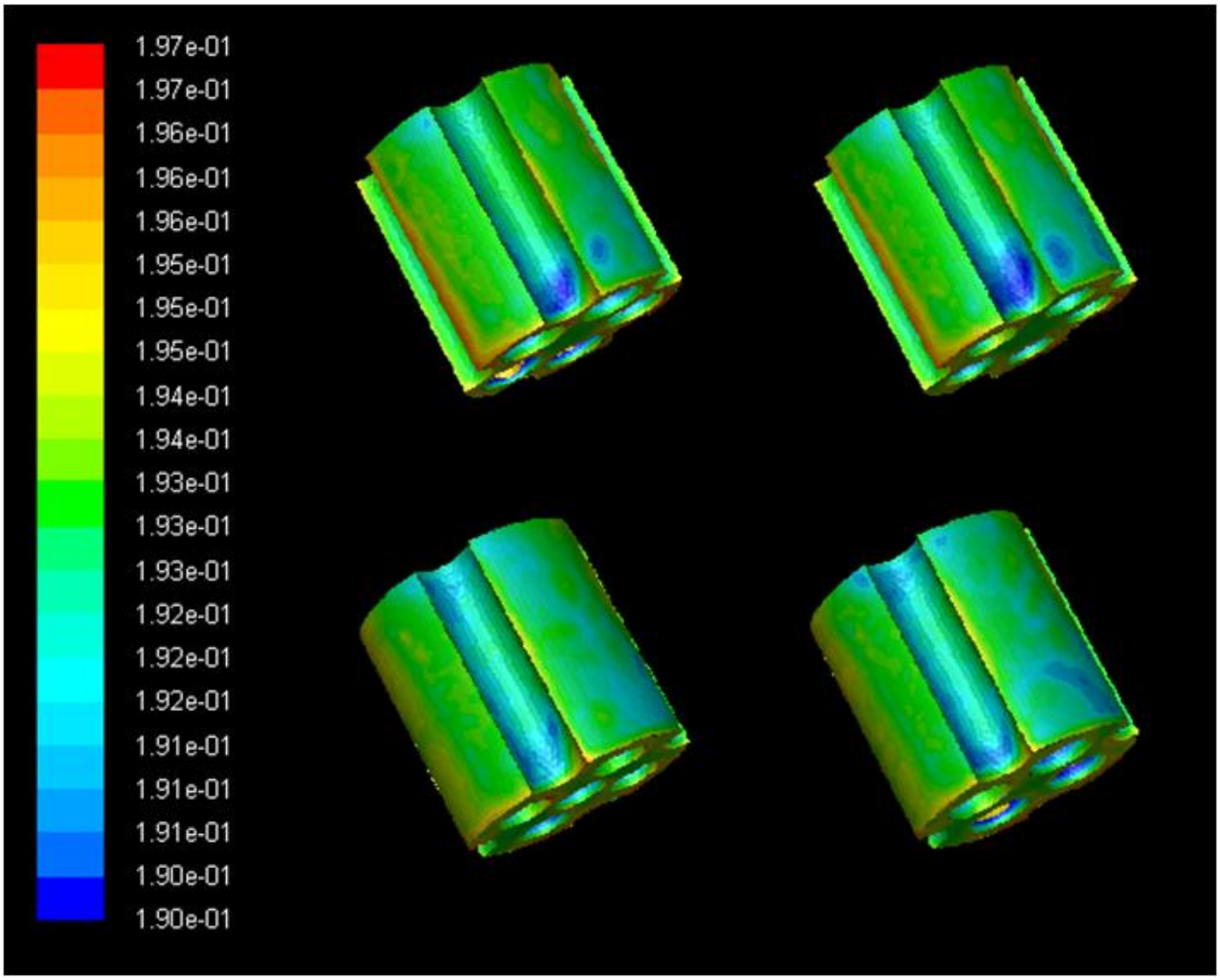

Figure 9: Methane mass fraction fields: top-left 5H-P, top-right 5H-P-small, bottom-left 5H-Q, bottom-right 4H-Q

The methane concentration on the surface of the particle affects the amount of reaction which occurs, since the reaction takes place on the surface of the catalyst. Since the rate of reaction is slightly dependent on the partial pressure of methane, it would be expected that the methane contours might roughly resemble the reaction rate contours. However, the areas of low methane, specifically within the groove, are in the same locations as high reaction areas. This implies that the concentration of methane has only a small effect on the reaction rate, and that temperature is much more of a controlling factor. This is observed by the similarities in the temperature and reaction rate plots from figures 6, 7, and 8.

The areas of high reaction noted above have relatively high methane concentrations according to the contour plots of Figure 9, however the areas of highest concentration are found near the particle

edges and on the bottom surface. This suggests that these areas should be reacting more, but are unable to for some reason. It is seen from the temperature plots that the bottom surface of the particles are very cool, which would inhibit the reaction progressing, but the edges of the particle grooves have a warmer temperature (not as hot as the intense hotspots), which would suggest that the reaction should progress at a higher rate, depleting the methane concentration in that area.

FLOW FIELD COMPARISONS

In order to further analyze the points made above, it is necessary to look at the flow profiles of each model and attempt to correlate flow features to the various anomalies found. The area in question is the flow field between the test particle and the partial one directly below it. The flow fields for each case can be seen in Figures 10 a-c. Each field ranges from velocities between 0 and 12 meters per second and the two solid particles can be seen to aid in visualizing the exact location of pathlines.

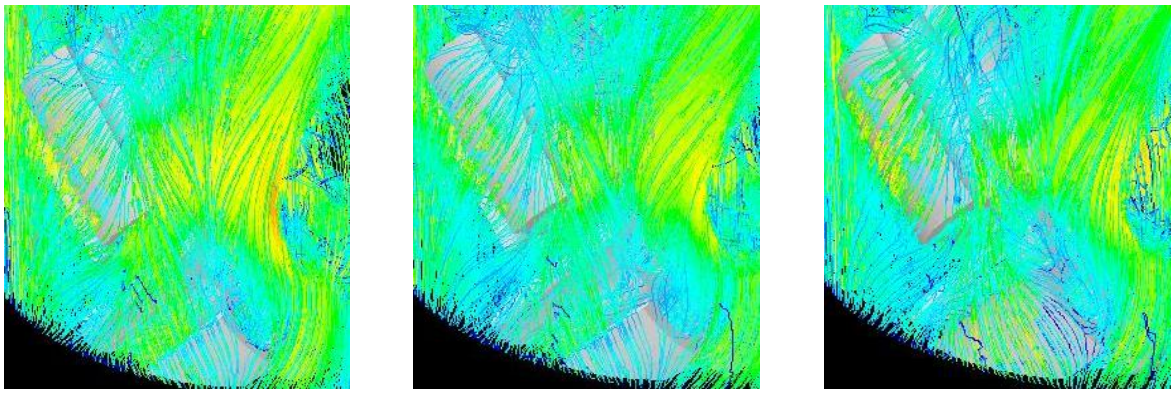

a) b) c)

Figure 10: Velocity pathlines in test particle vicinity: a) 5H-P b) 5H-P-small c) 5H-Q

The flow fields in both 5H-P geometries have higher velocities in general than the 5H-Q geometry, which can explain why the surface temperature is slightly lower in the 5H-P case. However, the increased flow should theoretically replenish methane along the surface of the test particle. This is not seen in Figure 9 which shows the 5H-P contains a lower mass fraction of methane within the visible groove. The remaining methane contours agree with increased flow in the 5H-P case as the mass fractions are generally higher. Although the 5H-P-small has slightly less flow in this area, the contours of Figure 9 show slightly higher concentrations of methane in the small holed case. This can be explained in a simple fashion. Due to the 5H-P geometry having larger holes, covering over 40% of the bottom face area, fluid flowing in the direction of the test particle has a much higher probability of being drawn inside the holes than in the smaller-holed case, in which the holes cover slightly less than 30% of the area. This causes more flow to be directed along the outer surface of the 5H-P-small particle, replenishing the methane concentration to a higher value.

To further illustrate this point, the methane contours for the surfaces inside the holes of each 5H-P geometry are shown below in Figure 11.

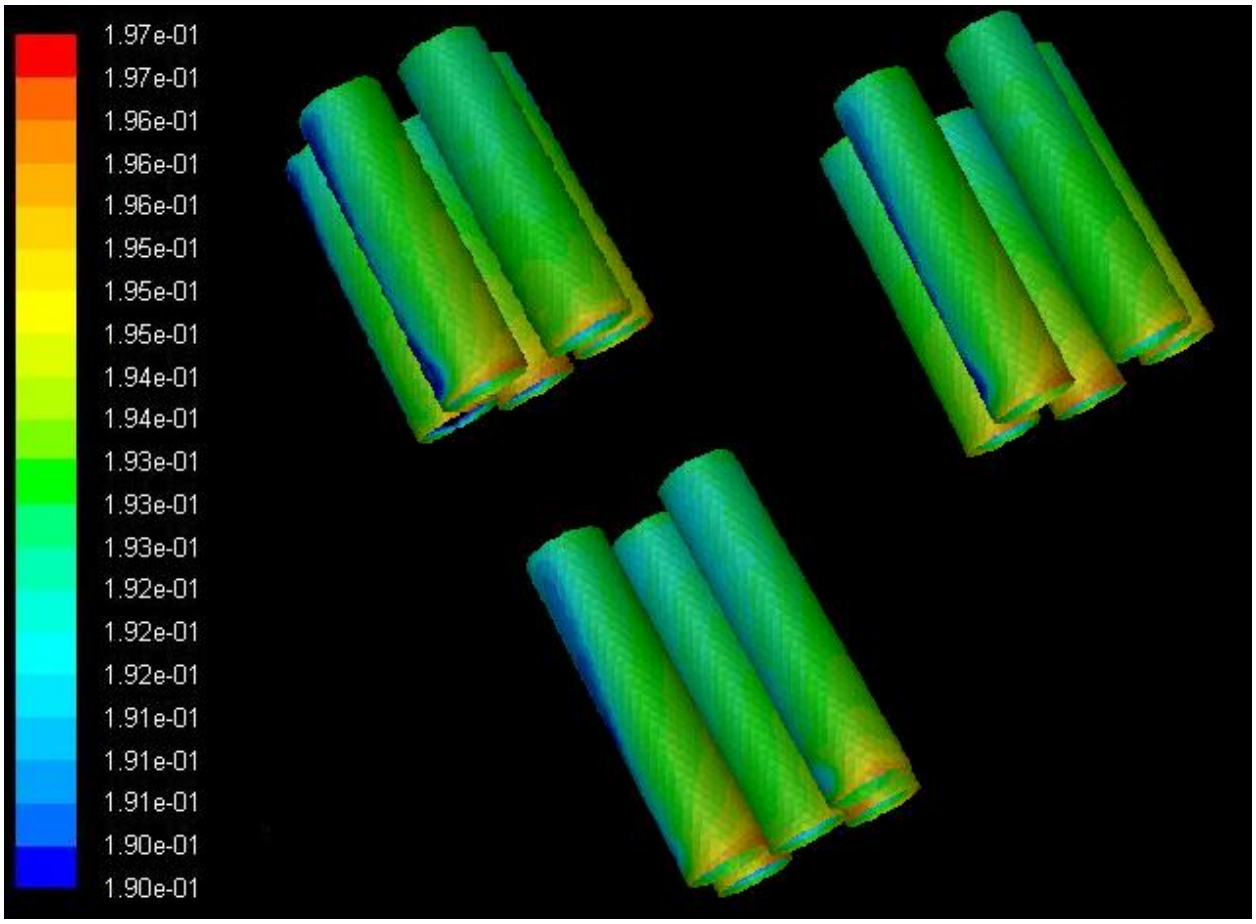

Figure 11: Inner hole surface methane contours: top-left 5H-P; top-right 5H-P-small; bottom 5H-Q

While the methane concentrations are nearly identical at the hole entry points (bottom), the concentration of methane quickly diminishes in the Q geometry due to lack of flow. The methane in the fluid is removed quickly to replenish surface sites over the first half of the hole length. However, the increased flow seen in the P geometries results in replenished methane concentration throughout nearly the entire particle length. This results in a much higher concentration on the inner surface of the particle in this case.

Of note also is that although the P geometries show high concentrations on average within the hole lengths, the portion of the surfaces nearest the tube wall (at the left) are much lower than in the Q geometry. Due to the holes being closer to the outer edge of the particle in the P case, it is likely than the temperature in the low methane regions is higher. This would result in higher reaction rates, which depletes methane more rapidly. Also consider that this portion of the hole is toward the "bottom" of the fluid flow path. It may be that as the mixture flows through the holes, it tends to replenish methane on the "top" of the hole, or on the right edge in Figure 11. This would result in lower concentrations along the left edges of the holes in the 5H-P geometry.

In addition to the features described above, the flow field also shows that the grooves help to funnel flow along the outer faces of the particle wall. This phenomenon was also observed in the study of the 4Q case and further explains why grooved geometries result in a higher tube wall temperature. It is known that with increased radial flow, convective heat transfer in the area of the tube wall is more efficient, reducing the tube wall temperature. However additional grooves cause the flow to funnel along the particle length, reducing the amount of radial flow at the tube wall. This leads to a higher average tube wall temperature and additional thermal stress on the reactor as a whole.

To reinforce this point numerically, one can refer to Table 6. By comparing the 4-hole grooved (4Q) model with the 5H-P-small model, the void fractions are similar. Trends shown prevously[7] stated that tube wall temperature correlates positively with void fraction. Thus, one naturally expects the wall temperature to be lower in the 5H-P-small case. However this is not true, even with smaller holes in the 5H-P-small model, which would normally increase radial flow. Due to the presence of an additional groove, the flow is directed more along the length of the particle than toward the tube wall. Furthermore, the 5H-Q model, which has about the same void fraction as the 5H-P-small case, has a lower tube wall temperature due to having one less groove. This forces more flow toward the tube wall, resulting in slightly better convective heat transfer.

The particle surface temperature is also affected by the changing geometry. By adding an additional hole to the particle, the chance of flow being pulled inside the “void space” in the particle is higher, and since the flowing gas is generally warmer than the pellet’s reacting temperature, the average surface temperature rises as a result of increased flow. This consequently increases reaction rates due to dependence on temperature given by the Arrhenius equation and the fact that the reaction has a positive activation energy. In addition the equilibrium favors more conversion of reactants at higher temperature because of its endothermic nature.

However, the orientation of the holes also affects the value of surface temperature. Between the 5H-Q and 5H-P-small cases, there is a significant discrepancy in surface temperature for the test particle. This results from the layout of holes. By placing holes toward the outer of the particle, flow which impacts the particle surface is generally in the center of the bottom face. Assuming the flow then has an equal probability of travelling in any direction along the face of the particle, there is a very high chance that it will encounter a hole, in which case the flow is likely to be pulled in. However, the solid surface in the 5H-Q case is located near the outer edge, as the holes are toward the middle including one in the center. Flow impacting the solid surface will be more likely to simply scatter away from the holes, and travel away from the particle. Figure 12 gives a visual representation of this phenomenon.

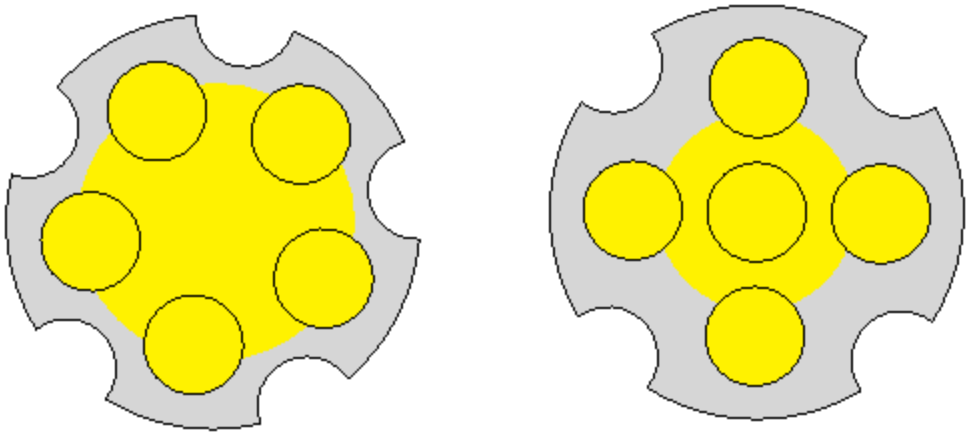

Figure 12: Comparison of hole layouts. left 5H-P-small, right 5H-Q

The areas in Figure 12 highlighted in yellow simply conceptualize the areas in which flow will tend to be drawn toward one or more holes in the geometry and do not follow from any calculations. The 5H-P-small geometry was selected for comparison because it has the same hole diameter as the 5H-Q case. It is quite clear that assuming a relatively similar volumetric flow approaches these two surfaces, the P orientation of holes will result in a much higher flow through holes, whereas the Q orientation will cause more flow to be directed in a radial manner. This should result in higher tube wall temperature for the P case, but also higher methane mass fractions as the increased flow tends to replenish the methane surface concentration.

In order to determine the cause of the second temperature hotspot in the 5H-Q geometry, velocity contours in the area were observed. A plane was selected through the highest intensity zone of the 5H-Q hotspot and is shown in Figure 13a. Figure 13b which follows depicts the velocity contours for each model at that plane.

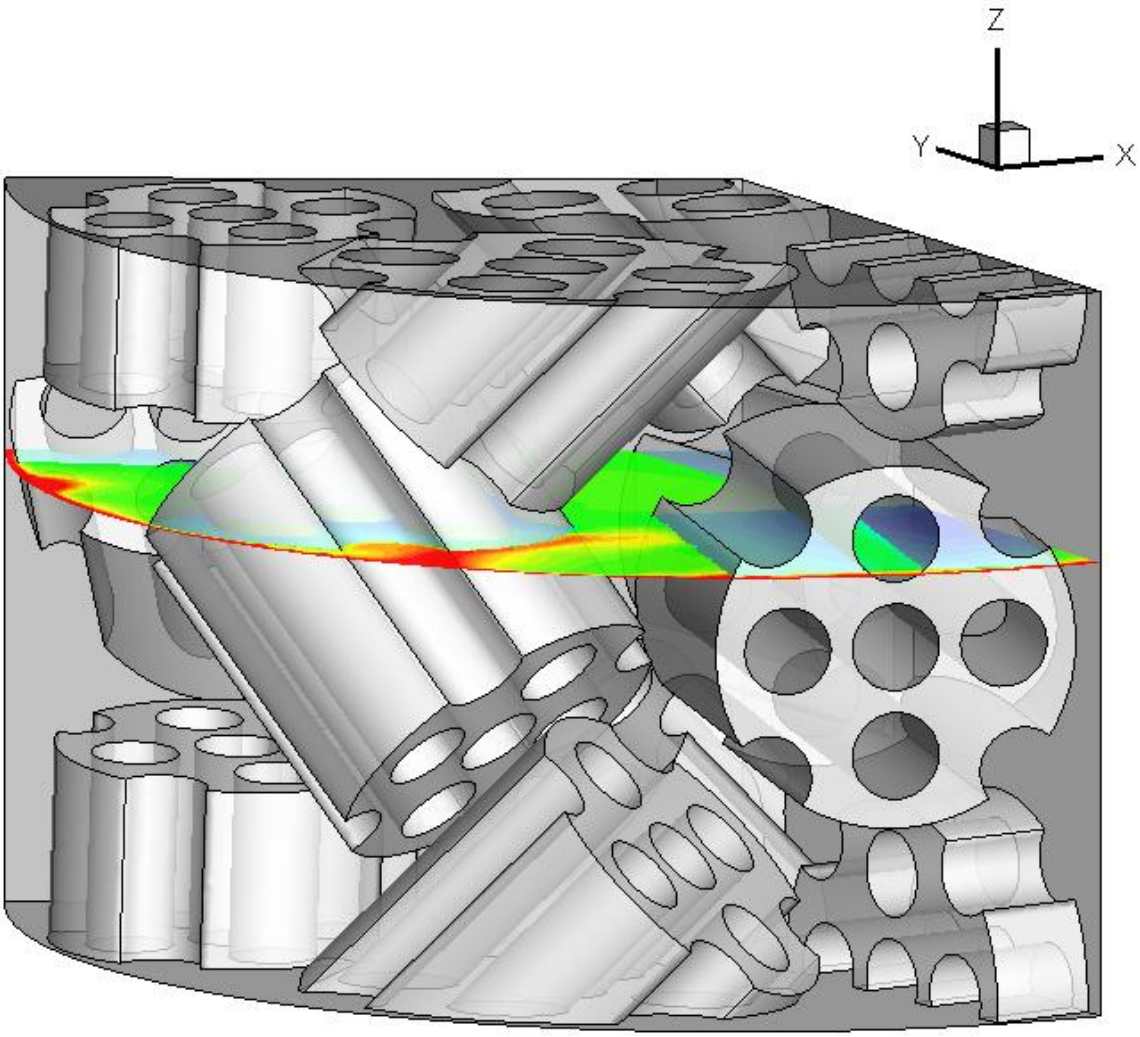

Figure 13a: Plane of interest at second temperature hotspot

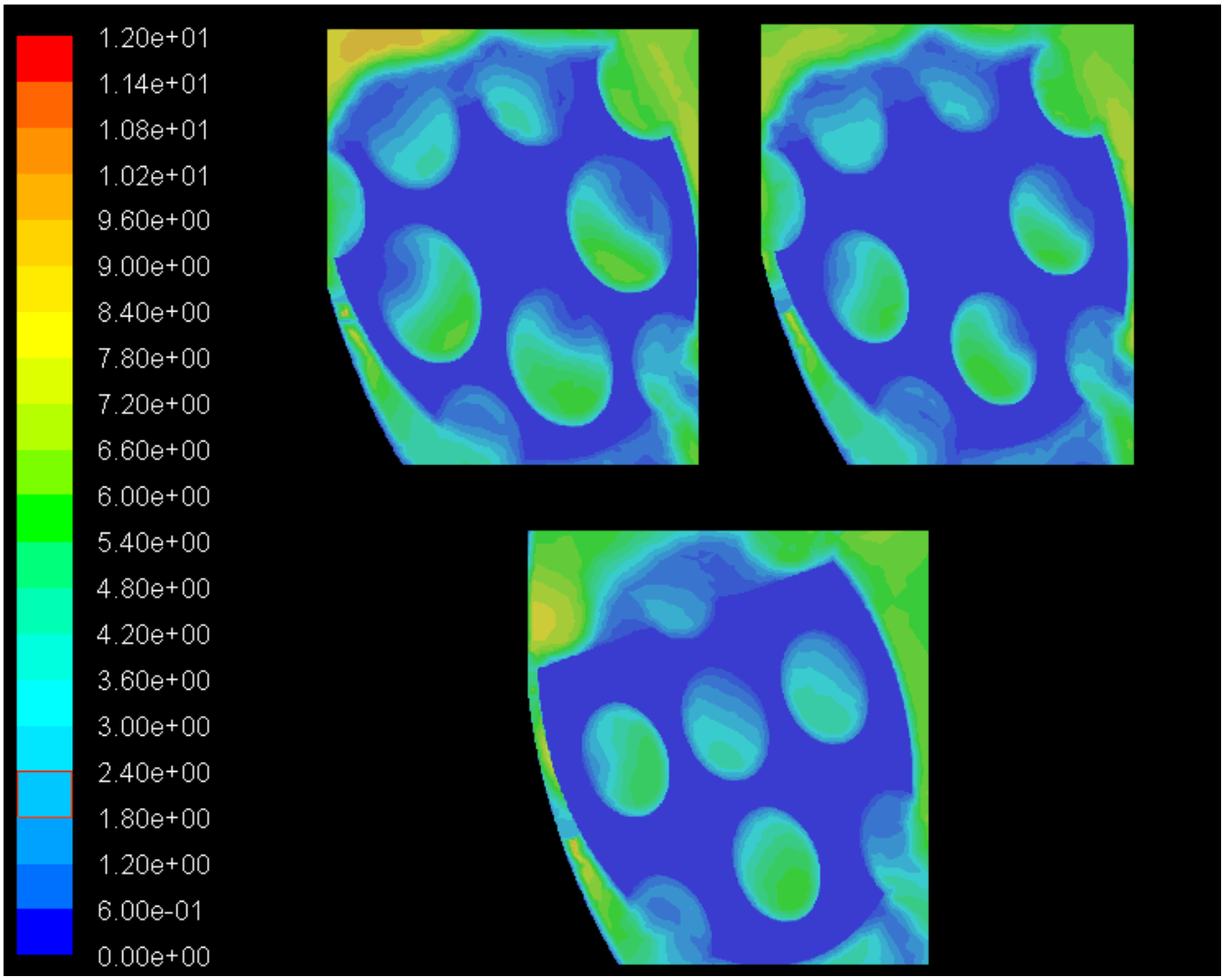

Figure 13b: Velocity contours at specified plane: top-left 5H-P; top-right 5H-P-small; bottom 5H-Q

Upon first inspection, the contours immediately support one result. It can be seen clearly that a much higher velocity of flow is observed within the holes of the 5H-P geometries. This indicates that more flow is pulled through the holes with this orientation compared with the 5H-Q geometry.

This is necessary to point out first as it increases radial mixing in the reactor wedge. This leads to more efficient convective heat transfer in the fluid bed, and a higher bulk flow temperature near the tube wall. Therefore, even though the flow velocity may be lower in the vicinity of the hotspot in the 5H-Q case, the higher bulk temperature results in a higher surface temperature for that geometry. To show this, the temperature contours for each model at the same plane are depicted below in Figure 14

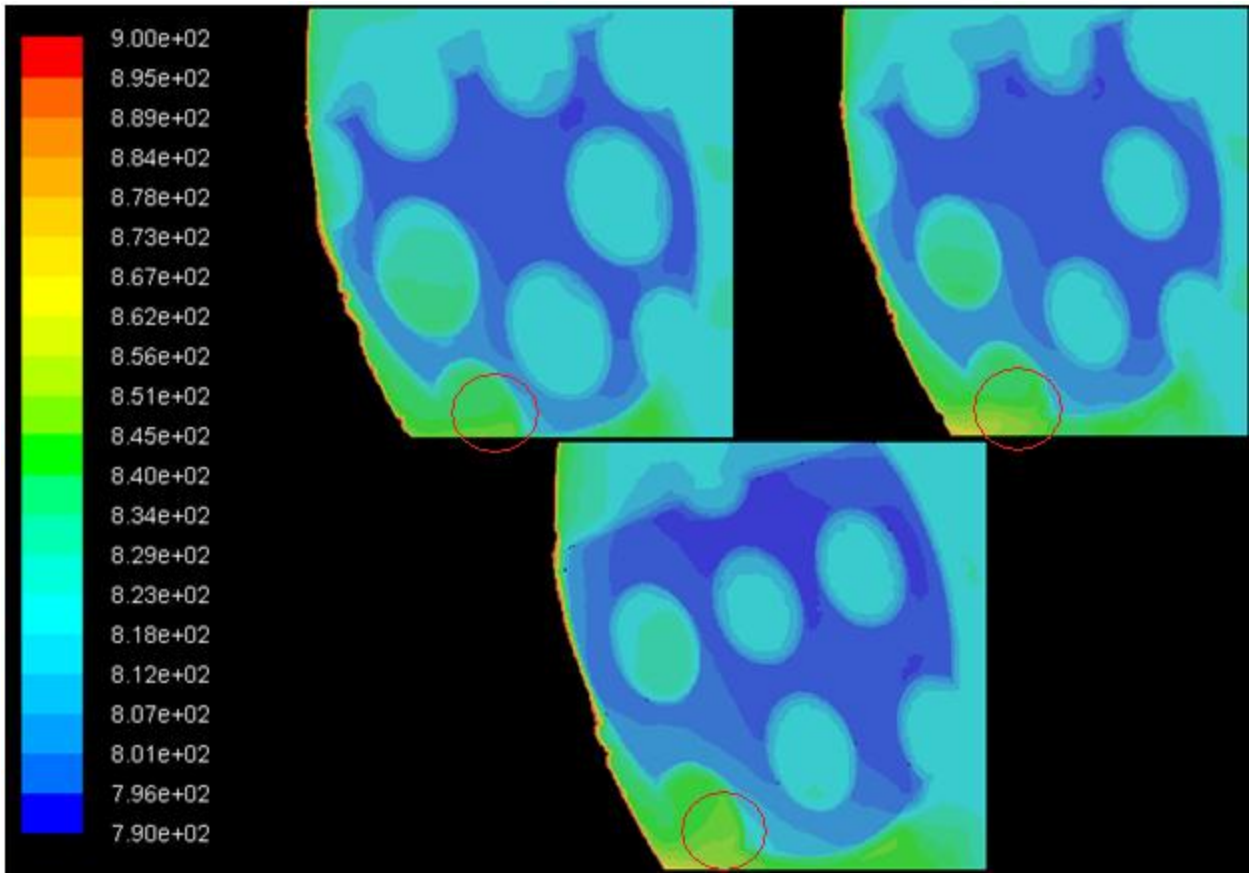

Figure 14: Temperature contours at specified plane. top-left 5H-P; top-right 5H-P-small; bottom 5H-Q

The temperature contours here are instrumental in showing why the hotspot exists more visibly in the 5H-Q case. The area outlined in red within Figure 14 is much warmer (about 15K) in the Q geometry than in either P case. This temperature is also about the same magnitude as the hotspot in the surface temperature hotspot in Figure 6.

Since this results from increased radial flow and convective heat transfer, it stands to reason that this phenomenon explains why the surface temperature in the 5H-Q case is higher near the tube wall than in the 5H-P models. The higher temperature also results in the observed reaction rate discrepancies, which are higher in the 5H-Q case as well.

CONCLUSIONS AND RECOMMENDATIONS

The goal of this project was to assess the feasibility of 5-holed cylindrical geometries for implementation as catalysts in steam methane reforming reactors. The hope was that these geometries could be used to further enhance already existing processes in terms of overall reactor performance. This specific study expands on previous studies of the following other multi-holed geometries: single hole, 3-holed, 4-holed (with and without cylindrical grooves), and 6-holed. This was achieved through a computational flow dynamics analysis of a reactor wedge model which approximates actual reactor operation. [7]

First, the results for the wall segment as a whole were studied. A defined pressure drop of 3,376 Pa/m was specified for the flow-only runs, and results from reaction-enabled runs showed that actual pressure drops varied within about 6% of this value, with the least accurate being the 5H-P case at 3167 Pa/m due to its slightly higher void fraction. There were some important trends to note in the results shown from the wall segment (Table 6). First, mass flow rate is increased with increasing void fraction due to increased volumetric fluid flow in the reactor bed. Compared with previous studies[7], the general trend of decreased exiting gas temperature with increased void fraction is followed, which is due to higher mass flow rates.

The changing of hole diameter within the 5H-P case did not yield any significant changes, better or worse. This suggests that for the most part, the behavior of the system is dependent more on the number and placement of holes, rather than their size. In general, larger holes would be preferred since it increases void fraction and thus mass flow rate in addition to lowering pressure drop. These also result in higher geometric surface area and reduced costs for operation.

Following, the results for the test particle were analyzed. It was observed that as particle surface area increased, the amount of reaction increased proportionally. However, due to much more efficient radial heat transfer in the 5H-Q case, surface temperatures and reaction rates per surface area are higher than in other geometries, though not by a large magnitude. This resulted from a higher bulk flow temperature around the test particle near the tube wall, which heated the particle surface, resulting in higher reaction rates. Increased flow also replenished the methane concentration more efficiently on the particle surface, allowing additional reaction to take place. Energy balance was confirmed by comparing the particle heat sink to FLUENT calculated heat fluxes on the particle surface area. In each case, the energy balance closed within 1%, as did mass balance across the top and bottom regions of the model. Particle mass balance was confirmed by measuring reaction rates and comparing these to calculated methane flows into and out of the test particle surfaces.

Overall, it has been determined that the 5H-Q geometry results in the highest reaction rates per surface area, but does not contain the high surface area of the 5H-P geometry due to requiring smaller hole to particle diameter ratio. Compounded with the lack of a 5th groove the 5H-Q geometry has a significantly reduced void fraction which results in mass flow being reduced by almost 3%. This combination of factors leads to selecting the 5H-P geometry as most suited to replace any catalyst geometry used in operations now as it has the highest overall reaction rates and a slightly lower tube

wall temperature than is observed in the 5H-Q geometry. This will over time result in the highest conversion of methane to hydrogen, which is the end purpose of the reactor.

However, it is likely that the 5H-Q geometry may produce better results if hole and/or groove size were increased. Due to the placement of geometrical entities in the 5H-Q case, there is significant room to increase the diameter of the cylindrical grooves. This would in turn increase the available surface area for reaction, as well as void fraction and mass flow rate. The 5H-P geometry studied does not have nearly as much additional space for increasing the diameter of either hole or grooves without beginning to compromise the structural integrity of the pellet, so it is likely optimized for this particle configuration.

Compared with previous results[7] the 5H-P is comparable to the 4-Q model. The reaction rates observed are slightly lower in the 5H-P case, but the increased void fraction results in a much higher flow rate with a very small increase in tube wall temperature of 2K. The surface area is much higher in the 5H-P case, so if more efficient catalyst materials are developed, the amount of reaction sites is highly increased over the 4-Q geometry. Combined with a high mass flow rate, this can be a very effective geometry for methane steam reforming processes.

REFERENCES

1. Simbeck DR. Hydrogen costs with CO2 capture. Presented at the 7th international conference on greenhouse gas control technologies (GHGT-7), Vancouver, British Columbia, Canada, September 6–10; 2004.

2. Stitt, E. (2005). Substainable strategies for the upgrading of natural gas. *NATO Science Series II Mathematics, Physics, & Chemistry , 191*, 185-216.

3. Kolaczkowski, S., Chao, R., Awdry, S., & Smith, A. (2007). Application of a CFD code (Fluent) to formulate models of catalytic gas phase reactions in porous catalyst pellets. *Chemical Engineering Research and Design , 85*, 1539-1552.

4. Hou, K., & Hughes, R. (2001). The kinetics of methane steam reforming over a Ni/a-Al2O catalyst. *Chemical Engineering Journal* , 311-328.

5. Menter, F., Kuntz, M., & Langtry, R. (2003). Ten years of industrial experience with the SST turbulence model. *Proc of the 4th International Symposium on Turbulence, Heat and Mass Transfer*, 625-632.

6. Doctor & Molburg. “Hydrogen from Steam-Methane Reforming with CO_2 Capture.” Presented at the 20th International Pittsburgh Coal Conference Sept. 15-19, 2003.

7. Boudreau, Justin & Rocheleau, Anne. “Comparison of Catalyst Geometries Using Computational Flow Dynamics for Methane Steam Reforming.” April 2010

8. “Steam Reforming of Natural Gas.” Accessed March 25, 2012. http://wiki.uiowa.edu/display/greenergy/Steam+Reforming+of+Natural+Gas

9. Dixon, A.G., Taskin, M.E., Nijemeisland, M., and Stitt, E.H., "A CFD Method to Couple 3D Transport and Reaction in Fixed Bed Catalyst Pellets to the External Flow Field", *Ind. Eng. Chem. Res.*, **49**, 9012 (2010).

10. Taskin, M.E., Dixon, A.G. and Stitt, E.H., "CFD Study of Fluid Flow and Heat Transfer in a Fixed Bed of Cylinders", *Numerical Heat Transfer A*, **52**, 203 (2007).

11. Birdsall, David James, et al. 2011. Shaped Heterogeneous Catalysts. U.S. Patent 0,172,086, filed August 24, 2009, and issued July 14, 2011.

12. Petelin, Stojin & Vidmar, Peter. “Application of CFD Method for Risk Assessment in Road Tunnels.” Engineering Applications of Computational Fluid Dynamics Volume 1, 273-287. (2007)

13. Taskin, M.E., Troupel, A., Dixon, A.G., Nijemeisland, M., and Stitt, E.H., "Flow, Transport and Reaction Interactions for Cylindrical Particles with Strongly Endothermic Reactions," Ind. Eng. Chem. Res. 49,9026 (2010).

APPENDIX A: Particle Locations in GAMBIT Geometry[8]

Particle	Orientation 1b	Orientation 2	Orientation 3
1	R +45 +x T -1.45 +x R +40 +z	R +90 +y T -1.42 +x T +1 +z R +30 +z	R +90 +x T -1.42 +x T +1 +z R +30 +z
2	R -45 +x T -1.45 +x T +1 +z R +20 +z	R +90 +x R +30 +z T +1 +z T +0.5 +y T -1.17 +x	h = 0.98 T -1.48 +x R +45 +z
3	**1** C +2 +z	h = 0.98 T -1.48 +x R +5 +z	**2** C +2 +z
4	R +5 +x T -1.48 +x R -9 +z	**3** C +2 +z	R +45 +x T -1.45 +x T +1 +z R -25 +z
5	**4** C +2 +z	R +90 +x T -1.42 +x R +55 +z	R -45 +x T -1.45 +x R -5 +z
6	R +90 +y T -1.42 +y R +5 +z	**5** C +2 +z	**5** C +2 +z
7	**6** C +2 +z	h = 0.98 T -1.48 +x T +1 +z R +75 +z	R +45 +x T -1.45 +x T +1 +z R +85 +z
8	R +90 +x T -1.42 +y T +1 +z R -17.5 +z	h = 0.98 T +1 +z T -0.2 +y T -0.35 +x	R -45 +x T -1.45 +x R +105 +z
9	R +45 +x T -1.45 +x T +1 +z R -40 +z	R +90 +x R +40 +z T -0.18 +y T -0.25 +x	**8** C +2 +z
10	R +90 +y T -0.25 +x	**9** C +2 +z	r = 0.49 R +90 +y T +1 +z T -0.25 +x
11	**10** C +2 +z	R +45 +x T -1.45 +x R -50 +z	R +90 +x R +30 +z T -0.25 +x T -0.25 +y
12	R +90 +x T +1 +z T -0.35 +y T +0.2 +x	**11** C +2 +z	**11** C +2 +z

R = rotate, T = translate, C = copy, h = adjust height to, r = adjust radius to. Rotations are in degrees, translations in inches. Based on particle of 1 inch diameter, 1 inch height

APPENDIX B: Boundary Layer Information

B.1: 5H-P Boundary Layers

Particle	First layer thickness (inches)	Growth	Number of layers	Total depth (inches)
Wall Boundary Layer				
N/A	0.001	1	2	0.002
Inner Boundary Layers (into the particle)				
2	0.003	1	2	0.006
Outer Boundary Layers (into the fluid)				
1	0.001	1	2	0.002
2	0.001	1	3	0.003
3	0.001	1	2	0.002
4	0.001	1	2	0.002
5	0.001	1	2	0.002

B.2: 5H-P-small Boundary Layers

Particle	First layer thickness (inches)	Growth	Number of layers	Total depth (inches)
Wall Boundary Layer				
N/A	0.001	1	2	0.002
Inner Boundary Layers (into the particle)				
2	0.003	1	2	0.002
Outer Boundary Layers (into the fluid)				
1	0.001	1	2	0.002
2	0.001	1	3	0.003
3	0.001	1	2	0.002
4	0.001	1	2	0.002
5	0.001	1	2	0.002

B.3: 5H-Q Boundary Layers

Particle	First layer thickness (inches)	\Growth	Number of layers	Total depth (inches)
Wall Boundary Layer				
N/A	0.001	1	2	0.002
Inner Boundary Layers (into the particle)				
2	0.005	1	2	0.01
Outer Boundary Layers (into the fluid)				
2	0.001	1	3	0.003
4	0.001	1	2	0.002
5	0.001	1	2	0.002

APPENDIX C: Sample GAMBIT Journal File

```
/ Journal File for GAMBIT 2.3.16, Database 2.3.14, ntx86 SP2006032921
/ Identifier "5H-P"
/ File opened for write Sun Nov 13 15:59:45 2011.
identifier name "yournamehere" new nosaveprevious
solver select "FLUENT 5/6"
reset
/
////////////////////////////////////////////////////////////////////////////
/                    Geometry creation                                     /
////////////////////////////////////////////////////////////////////////////
/
volume create "cylinder" height 2 radius1 2 radius2 2 radius3 2 offset 0 0 1 \
  zaxis frustum
volume create "part" height 1 radius1 0.5 radius3 0.5 zaxis frustum

/Insert Details of specific geometry in this area/

volume copy "part" to "part1"
volume move "part1" dangle 45 vector 1 0 0 origin 0 0 0
volume move "part1" offset -1.45 0 0
volume move "part1" dangle 40 vector 0 0 1 origin 0 0 0
volume copy "part" to "part2"
volume move "part2" dangle -45 vector 1 0 0 origin 0 0 0
volume move "part2" offset -1.45 0 0
volume move "part2" dangle 20 vector 0 0 1 origin 0 0 0
volume move "part2" offset 0 0 1
volume copy "part1" to "part3"
volume move "part3" offset 0 0 2
volume copy "part" to "part4"
volume move "part4" dangle 5 vector 1 0 0 origin 0 0 0
volume move "part4" offset -1.48 0 0
volume move "part4" dangle -9 vector 0 0 1 origin 0 0 0
volume copy "part4" to "part5"
volume move "part5" offset 0 0 2
volume copy "part" to "part6"
volume move "part6" dangle 90 vector 0 1 0 origin 0 0 0
volume move "part6" offset 0 -1.42 0
volume move "part6" dangle 5 vector 0 0 1 origin 0 0 0
volume copy "part6" to "part7"
volume move "part7" offset 0 0 2
volume copy "part" to "part8"
volume move "part8" dangle 90 vector 1 0 0 origin 0 0 0
volume move "part8" offset 0 0 1
volume move "part8" offset 0 -1.42 0
volume move "part8" dangle -17.5 vector 0 0 1 origin 0 0 0
volume copy "part1" to "part9"
```

```
volume move "part9" offset 0 0 1
volume move "part9" dangle -40 vector 0 0 1 origin 0 0 0
volume move "part9" dangle -40 vector 0 0 1 origin 0 0 0
volume copy "part" to "part10"
volume move "part10" dangle -45 vector 0 1 0 origin 0 0 0
volume move "part10" offset -0.25 0 0
volume copy "part10" to "part11"
volume move "part11" offset 0 0 2
volume copy "part" to "part12"
volume move "part12" dangle 90 vector 1 0 0 origin 0 0 0
volume move "part12" offset 0 0 1
volume move "part12" offset 0.2 0 0
volume move "part12" offset 0 -0.35 0
volume delete "part" lowertopology
volume create "b1" width 3 depth 3 height 4 offset 1.5 1.5 2 brick
volume move "b1" offset 0 0 -1
volume copy "b1" to "b2"
volume move "b2" dangle 60 vector 0 0 1 origin 0 0 0
volume copy "b1" to "b3"
volume move "b3" dangle -90 vector 0 0 1 origin 0 0 0
volume copy "b1" to "b4"
volume move "b4" offset -3 0 -3
volume copy "b4" to "b5"
volume move "b5" offset 0 -3 0
volume copy "b5" "b4" to "b6" "tool"
volume move "b6" "tool" offset 0 0 6
volume unite volumes "tool" "b6" "b4" "b5" "b2" "b1" "b3"
/ Modification to W geometry
volume move "tool" dangle -1 vector 0 0 1 origin 0 0 0
volume move "part1" "part2" "part3" "part4" "part5" "part6" "part7" "part8" \
  "part9" "part10" "part11" "part12" offset 0 0 0.04
/ Trim cylinder and the eleven particles that stick out of the segment
volume subtract "cylinder" volumes "tool" keeptool
volume subtract "part7" volumes "tool" keeptool
volume subtract "part3" volumes "tool" keeptool
volume subtract "part11" volumes "tool" keeptool
volume subtract "part5" volumes "tool" keeptool
volume subtract "part4" volumes "tool" keeptool
volume subtract "part1" volumes "tool" keeptool
volume subtract "part10" volumes "tool" keeptool
volume subtract "part6" volumes "tool" keeptool
volume subtract "part12" volumes "tool" keeptool
volume subtract "part8" volumes "tool" keeptool
volume subtract "part9" volumes "tool"
/Split cylinder with particles to avoid connecting faces
volume split "cylinder" volumes "part1" "part2" "part3" "part4" "part5" \
  "part6" "part7" "part8" "part9" "part10" "part11" "part12" connected
```

```
////////////////////////////////////
/Label all faces for future reference/
////////////////////////////////////

/Modify Face labels in order to refer to them later/

//////////////////////////////////////////
/           FACE LINKING                 /
//////////////////////////////////////////


/Link all faces on the top and bottom of the geometry to create periodic zone/

//////////////////////////////////////////
/     Boundary and Continuum Types      /
//////////////////////////////////////////

/Define Fluid/solid volumes and boundary types in this section/

//////////////////////////////////////////
/              BLs                       /
//////////////////////////////////////////

/Define Boundary Layer information for any boundary layers which are needed/

//////////////////////////////////////
/            MESH                    /
//////////////////////////////////////

/Input meshing details for geometry here/

/Write out the mesh
export fluent5 "yournamehere.msh"
```